Line Forces in Keplerian Circumstellar Disks and Precession of Nearly Circular Orbits

K. G. Gayley
Department of Physics and Astronomy, University of Iowa, Iowa City, IA 52242

R. Ignace
Department of Physics and Astronomy, University of Iowa, Iowa City, IA 52242

S. P. Owocki
Bartol Research Institute, University of Delaware, Newark, DE 19716

ABSTRACT

We examine the effects of optically thick line forces on orbiting circumstellar disks, such as occur around Be stars. For radially streaming radiation (e.g., as from a point source), line forces are only effective if there is a strong radial velocity gradient, as occurs, for example, in a line-driven stellar wind. However, we emphasize here that, within an orbiting disk, the radial shear of the azimuthal velocity leads to strong line-of-sight velocity gradients along nonradial directions. As such, we show that, in the proximity of a stellar surface extending over a substantial cone angle, the nonradial components of stellar radiation can impart a significant line force to such a disk, even in the case of purely circular orbits with *no* radial velocity.

Given the highly supersonic nature of orbital velocity variations, we use the Sobolev approximation for the line transfer, extending to the disk case the standard CAK formalism developed for line-driven winds. We delineate the parameter regimes for which radiative forces might alter disk properties; but even when radiative forces are small, we analytically quantify higher-order effects in the linear limit, including the precession of weakly elliptical orbits. We find that optically thick line forces, both radial and azimuthal, can have observable implications for the dynamics of disks around Be stars, including the generation of either prograde or retrograde precession in slightly eccentric orbits. However, our analysis here suggests a net *retrograde* effect, in apparent contradiction with observed long-term variations of violet/red line profile asymmetries from Be stars, which are generally thought to result from *prograde* propagation of a one-arm, disk-oscillation mode. We also conclude that radiative forces may alter the dynamical properties at the surface of the disk where disk winds originate, and in the outer regions far from the star, and may even make low-density disks vulnerable to being blown off completely.

Subject headings: stars: atmospheres, early-type, emission-line, Be, winds

1. Introduction

Be stars are defined to be non-supergiant B stars that have shown emission in one or more Balmer lines at some time. As early as 1931, Struve had identified non-sphericity associated with rapid stellar rotation as the source for the Be star emission lines and profile shapes. Although the details have changed substantially, Struve's overall premise has withstood the test of time. Optical interferometry has conclusively shown that Be stars possess extended equatorial circumstellar disks that are geometrically thin, with the opening angle of the inner disk being of order a few degrees to be consistent with interferometric and polarimetric measurements (Quirrenbach et al. 1997; Wood, Bjorkman, & Bjorkman 1997).

Increasing observational evidence suggests that these circumstellar disks are in Keplerian orbit (e.g., Waters & Marlborough 1994; Hummel & Vrancken 2000). For example, Keplerian disks have been shown to be capable of supporting one-armed spiral density modes, whereas an angular-momentum conserving disk will not (Okazaki 1991, 1996, 1997). These one-armed modes result in a non-axisymmetric disk structure that is supported by observations (Telting et al. 1994; Hanuschik et al. 1995; Hummel & Hanuschik 1997).

The one-armed pattern is also typically observed to precess around the disk. It has long been known that some Be stars that show violet (V) and red (R) peaks with a central depression in the Hα emission line can undergo quasi-periodic variations in the relative strengths of these peaks (e.g., Dachs 1987; Hubert 1994). This cyclic behavior is commonly referred to as "V/R variations" with typical periods of years to decades (e.g., see the compilation in the Appendix of Okazaki 1997). The V/R variations are thought to result from the prograde precession of "Global Disk Oscillations" (GDOs) in Keplerian Be disks (Papaloizou, Savonije, & Henrichs 1992; Telting et al. 1994; Hanuschik 1994; Mennickent, Sterken, & Vogt 1997). Measurements with optical interferometry have now confirmed the non-axisymmetric disk structure in ζ Tau and γ Cas, and have even observed the slow secular motion of the pattern around the star (Vakili et al. 1998; Berio et al. 1999).

However, there are numerous outstanding concerns in relation to Be disks and GDOs. It is unclear exactly how the Keplerian disks are generated, and two well-studied Be stars (λ Eri: Smith et al. 1993; and γ Cas: Robinson & Smith 2000; Cranmer, Robinson, & Smith 2000), show evidence for flaring activity and co-rotating clouds of gaseous material that are interpreted as signatures of magnetic fields. Furthermore, several Be stars are observed to

be non-radial pulsators, and so variations in temperature and brightness across the face of the star might affect the disk structure. Finally, the GDO behavior is actually only quasi-periodic, and sometimes the V/R variations can change period, appear, or disappear entirely. Even the entire circumstellar disk can "disappear", only to be regenerated at a later time. For example the disk in the Be star μ Cen appears to be "rebuilding" itself (Rivinius et al. 1998), at a rate consistent with stellar mass loss (Telting et al. 1998). The lack of a clear explanation for such curious behavior suggests that the study of Be stars is in a phase where all the relevant physics is still being assembled, and all potentially important contributors must be considered.

In this spirit, we consider here a process that has been generally overlooked: the potential impact of *optically thick line* forces on Keplerian disks and GDOs. In the past, GDO models have either ignored radiative forces (e.g., Papaloizou, Savonije, & Henrichs 1992) or assumed that the radiative line driving force is purely radial and derives entirely from optically thin lines (e.g., Okazaki 1997, which adopts the purely parametric prescription of Chen & Marlborough 1994). However, since the line force is affected by the strong velocity shear present in a Keplerian disk, the highly supersonic orbital speed effectively broadens optically thick lines. Much as in stellar winds, this can have important dynamical consequences.

To understand how a Keplerian disk generates line-of-sight velocity gradients, consider the schematic in Figure 1. The key point is that the finite size of the star allows for nonradial radiation streams, including the tangential stream from the limb depicted in the figure. These streams encounter the disk at oblique angles that sample the Keplerian velocity gradient, even in the absence of any radial motions. Since the Keplerian speeds are of the same order of magnitude as wind speeds, and they vary over the same scale, the line-of-sight gradients can also be of the same order for favorable geometries. Thus the geometric differences between applying CAK-type line forces (Castor, Abbott, & Klein 1975) to winds and disks are not as large as has been assumed in the past, and indeed the primary difference will be shown to be related to the density contrast, not the geometry.

The magnitude of the line-driving force cannot dominate the overall gravitational binding if disks are to exist in steady state. However, it can readily compete with the relatively weak forces commonly included in models of higher-order disk dynamics, in which GDO precession is controlled by pressure and nonspherical corrections to the stellar gravity (Okazaki 1997; Mennickent, Sterken, & Vogt 1997). Previous models have aleady found that the form of the linearized GDO solution can be altered by optically thin line-forces, thus leading to different responses in early- and late-type Be stars (Okazaki 1997, 2000). Here we provide a substantially more general treatment of disk line forces, built upon the formalism developed Castor, Abbott, & Klein (1975) to model line-driven stellar winds.

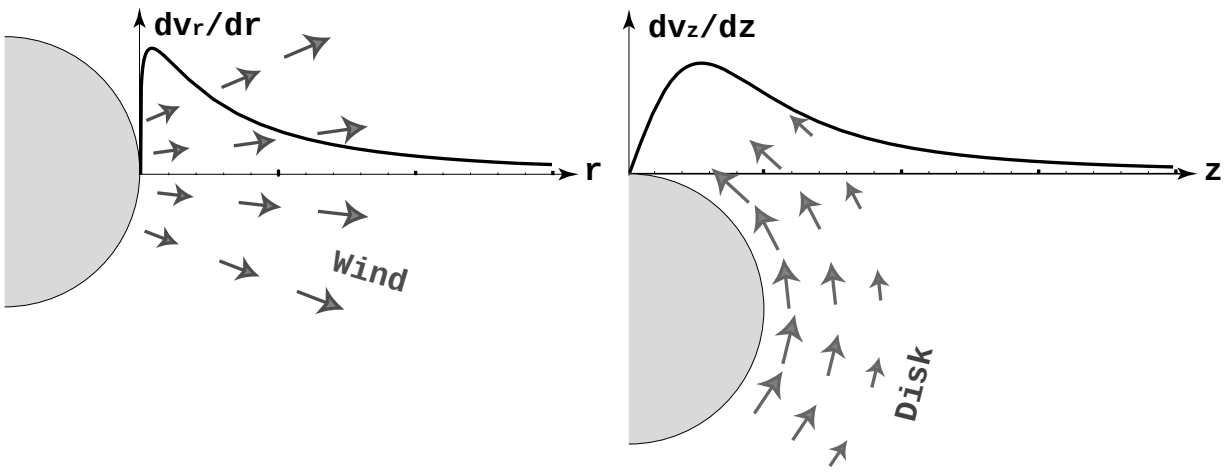

Fig. 1.— Comparison of the radial velocity gradient, dv_r/dr, of a radial stellar wind outflow with the line-of-sight gradient, dv_z/dz, along a ray direction z that is *tangent* to the stellar limb and passing through an orbiting Keplerian disk. The units of the gradient are arbitary, but the relative scaling is accurate for the case in which the terminal velocity of the wind is the same as the near-surface orbital velocity of the disk. Note that, even without any radial outflow, the gradients are quite comparable. This represents a key factor in the potential for line-forces to be important in orbiting disks as well as outflowing winds.

Although this paper only specifically treats cricumstellar disks around hot stars, the formalism may be applicable to other UV-bright disk environments, such as accretion disks in cataclysmic variables (Drew & Proga 2000; Feldmeier, Shlosman, & Vitello 1999). Another potentially important analogy is with accretion disks thought to exist in active galactic nuclei. Recently, line forces in such disks have been considered by Proga, Stone, & Kallman (2000), and such work can also benefit from the analytic perspective taken in this paper, tailored to that alternate context.

In §2, we describe our approach for extending the CAK line-force formalism to the case of a Keplerian disk, and then in §3 estimate the magnitude of the resulting forces for a range of model parameters. These estimates are often small compared to the radial force scale set by gravity, and so in §4 we investigate in the linear limit the higher-order effect on low-amplitude disk perturbations, deriving the precession for a homologous family of slightly eccentric orbits. The conclusions of how line forces affect low-density regions of the disk and the precession rates of nearly circular orbits are given in §5. An Appendix gives the details of the analytic calculation of the precession period.

2. Treatment of Line Forces

Within the context of the above introduction, let us now lay the basis for quantifying line forces in Keplerian disks. The essential physics of supersonic line driving involves the Doppler shifting of lines into resonance with stellar continuum photons over a narrow region of physical space. This allows each such line to be treated in the Sobolev approximation (Sobolev 1960), and the cumulative effect of the thousands of contributing lines can then be accomodated using the standard CAK formalism. This formalism is by now quite well established, and so we will merely cite the results relevant for the forces on gas parcels in nearly circular orbits in the equatorial plane, taking the geometric expressions derived in Cranmer & Owocki (1995) and using the nomenclature described in Gayley (1995).

To accomodate the effects of thousands of arbitrary lines, we follow a statistical approach equivalent to CAK. We fit the number of lines $\tilde{N}(q)$ with line strength greater than q with a power law over the domain of marginally thick lines, which is decisive for the line force. The line strength q is here given for line i to be

$$q_i \;=\; \frac{3}{8}\frac{\lambda_i}{r_e} a_i f_i \;, \tag{1}$$

where λ_i is the line wavelength, $r_e = e^2/mc^2$ is the classical radius of the electron, a_i is the abundance, relative to free electrons, of bound electrons in the lower level of the transition,

and f_i is the oscillator strength. The value of q may be interpreted as the force on the bound electrons, relative to the force on the free electrons, with no account taken for opacity effects that redistribute photons out of the absorbing bandwidth and limit the radiative acceleration.

To obtain the standard meaning of the CAK line-list parameter α, we assume

$$\tilde{N}(q) \;=\; \left(\frac{q}{Q}\right)^{\alpha-1} \quad , \tag{2}$$

where Q is simply a normalization constant that can be interpreted as the q of the apparent strongest line, if the power-law distribution is extrapolated from the domain of marginally thick lines into the realm of extremely thick lines. Note Q is not necessarily the q of the *actual* strongest line, which plays little role in the total radiative force. For readers familiar with prior literature in this area, note that it is more standard to define a *differential* line-strength distribution function, of which $\tilde{N}(q)$, having the meaning of an actual number of lines, is the integrated form.

This simple form for $\tilde{N}(q)$ yields for the radiative acceleration in vector notation (see e.g., Cranmer & Owocki 1996; Owocki, Cranmer, & Gayley 1996)

$$\mathbf{g} \;=\; \Gamma(\alpha) Q \frac{\kappa_{es}}{c} \int d\hat{n}\; \hat{\mathbf{n}} I(\hat{\mathbf{n}}) \left[\tilde{t}(\hat{\mathbf{n}})\right]^{-\alpha} \quad , \tag{3}$$

where we have introduced the line-shadowing parameter

$$\tilde{t}(\hat{\mathbf{n}}) \;=\; Q\rho\kappa_{es}c \left[(\hat{\mathbf{n}}\cdot\nabla)\,(\hat{\mathbf{n}}\cdot\mathbf{v})\right]^{-1} \quad , \tag{4}$$

where $\Gamma(\alpha)$ is the standard Gamma function. Note that $\tilde{t}$ can be thought of as the Sobolev optical depth of a line of strength Q. For a power-law line list, $\tilde{t}$ is of order the cumulative Sobolev optical depth along $\hat{\mathbf{n}}$ summed over all lines. When raised to the $-\alpha$ power and averaged over the directions of incident flux, $\tilde{t}$ incorporates all opacity effects and gives the self-shadowing reduction of the line force.

To connect with standard nomenclature, $\tilde{t}$ is the CAK parameter t multiplied by Qc/v_{th}, and unlike t itself, it is independent of both v_{th} and the Sobolev length. Indeed, neither of these latter parameters need even be specified here (as long as they are small), which circumvents certain ambiguities in the more standard notation.

2.1. The Vector Correction for Self-Shadowing

One particularly convenient way to incorporate the effects of line optical depth is to consider the ratio of the radiative force $\mathbf{g}$ to g_{thin}, the magnitude of the force if all lines were

optically thin (obtained by setting $\tilde{t} = 1$ in eq. [3] and considering only the magnitude). This ratio gives a vector result with a magnitude less than unity (often much less), which can be termed the vector correction for line shadowing and written as

$$\mathbf{P} \;=\; \frac{\mathbf{g}}{g_{thin}} \;. \tag{5}$$

In the absense of strict spherical symmetry, $\mathbf{P}$ is in general a *nonradial* vector. This holds even when the flux *is* radial; all that is required is an asymmetry in effective opacity caused by nonspherical flows, such as will be considered below.

To simplify the angular integrals for the purposes of this paper, we will assume a spherical star with no limb- or gravity-darkening, despite the likely possibility that both occur in reality. Also, the disk is assumed to be optically thin in the continuum, and photons are assumed to interact with at most one line, so the disk thickness and density are limited. With these assumptions, using equation (2) with an exponential cutoff at $q = Q$ (simply for purposes of defining g_{thin}) yields

$$\mathbf{P} \;=\; \frac{1}{\pi}\frac{r^2}{R^2}\int_{\mu_*}^{1} d\mu \int_0^{2\pi} d\phi \; \hat{\mathbf{n}}(\mu,\phi)\tilde{t}(\mu,\phi)^{-\alpha} \;. \tag{6}$$

Here μ and ϕ give respectively the direction cosine from the radius vector and the incident azimuthal angle of the photon, and $\mu_* = \sqrt{1 - R^2/r^2}$ gives the direction cosine to the limb.

In applications, it is often convenient to express the radiative force relative to gravity. This is normally done in terms of the Eddington parameter Γ, the ratio of the radiative force on free electrons to gravity (and is not to be confused with the Gamma function $\Gamma(\alpha)$). It then follows that

$$\mathbf{g} \;=\; g_{grav}\Gamma \; \frac{g_{thin}}{g_{es}} \; \mathbf{P} \;, \tag{7}$$

where the ratio of the radiative force on lines, without any shadowing correction, to the radiative force on free electrons is by our convention

$$\frac{g_{thin}}{g_{es}} \;=\; Q\Gamma(\alpha) \;. \tag{8}$$

Thus

$$\mathbf{g} \;=\; g_{grav}\Gamma Q \; \Gamma(\alpha) \; \mathbf{P} \tag{9}$$

provides a general and convenient expression for the radiative force for a statistical distribution of marginally optically thick lines in the Sobolev approximation.

A key assumption here is that equation (2) applies universally over the circumstellar medium, and so may be viewed as a global constraint. Radially dependent effects, such as

might be linked to gradients in ionization or temperature, are not explicitly included. By contrast, Chen & Marlborough (1994) neglected the optical depth effects controlled by the **P** vector, but instead allowed the line parameters to be radially varying in a parametric way, albeit without clear physical justification. Although a complete treatment must accomodate both shadowing by line optical depth and the radial gradients for an *actual* line list, for conceptual simplicity we choose to include only the former, because of the importance of the dynamical dependences it implies. Also, it is implicitly assumed that there are a large number of optically thick lines and a statistical treatment is justified, which also requires that $P_r \ll 1$. This is more likely to hold in a dense disk than in the weakest B-star winds (Babel 1996).

2.2. The Line-of-Sight Velocity Gradient in the Equatorial Plane

The above results are general and entirely equivalent to the standard CAK formalism with a fixed line-list parametrization. Since our present interest is orbiting disks, we will now consider the explicit restriction of these equations to that context. For simplicity we consider only forces in the equatorial plane. Then the dependence on the line-of-sight gradient of the line-of-sight velocity becomes (e.g., Batchelor 1967; Cranmer & Owocki 1995)

$$|(\hat{\mathbf{n}} \cdot \nabla)(\hat{\mathbf{n}} \cdot \mathbf{v})| \;=\; |H(\mu,\phi)| \tag{10}$$

where

$$H(\mu,\phi) \;=\; \mu^2 \frac{\partial v_r}{\partial r} \;+\; (1-\mu^2)\frac{v_r}{r} \;+\; \mu\sqrt{1-\mu^2}\sin\phi\left(\frac{\partial v_\phi}{\partial r} \;-\; \frac{v_\phi}{r}\right) \;, \tag{11}$$

and the correction for line shadowing becomes

$$\tilde{t}^{-\alpha} \;=\; (Q\rho\kappa_{es}c)^{-\alpha}\,|H(\mu,\phi)|^{\alpha} \;. \tag{12}$$

2.3. Radial Forces on Circular Orbits

Interactions between gas parcels favor orbital circularization. If circular orbits are assumed, the above expressions simplify considerably, since then

$$v_\phi = \sqrt{\frac{GM}{r}} \tag{13}$$

and so $\mathrm{d}v_\phi/\mathrm{d}r = -0.5\; v_\phi/r$ may be substituted into equation (11). The negative sign implies that the Keplerian velocity shear *augments* the gradient due to orbital curvature, thereby strengthening the magnitude of the effects we consider.

Setting $v_r = 0$ for circular orbits then gives

$$\tilde{t}(\hat{\mathbf{n}})^{-\alpha} \;=\; \left(\frac{3}{2}\right)^{\alpha} (Q\rho\kappa_{es}c)^{-\alpha}\,(GM)^{\alpha/2}\,r^{-3\alpha/2}\mu^{\alpha}(1-\mu^2)^{\alpha/2}|\sin\phi|^{\alpha}\;. \tag{14}$$

From equation (6) this in turn gives for the radial component of the self-shadowing correction

$$P_r \;=\; \frac{2}{\pi}\left(\frac{3}{2}\right)^{\alpha} R^{\alpha}\,(Q\kappa_{es}c)^{-\alpha}\,(GM)^{\alpha/2}\,\rho^{-\alpha}r^{-5\alpha/2}A_{\alpha}f_0(r)\;, \tag{15}$$

where we have defined for convenience the weakly varying order-unity expressions

$$A_{\alpha} \;=\; \int_0^{2\pi} d\phi\;|\sin\phi|^{\alpha} \tag{16}$$

and

$$f_l(r) \;=\; \frac{1}{4}\int_0^1 dx\;x^{\alpha/2}\left(1\;-\;\frac{R^2}{r^2}x\right)^{\alpha/2\;-\;l}\;. \tag{17}$$

Figure 2 plots the quantities $A_\alpha f_0$ and $A_\alpha(1.5 - f_1/f_0)$ (the latter will be needed below in §4), expressed as functions of r/R for selected α, to demonstrate their weak dependence on r. The figure shows that $A_\alpha f_0(r)$ is generally close enough to unity that conceptual results can safely omit this factor. The primary dependences are instead contained in the other factors in equation (15). Specifically, if the disk density falls steeply as $\rho \propto r^{-n}$, then the radial radiative force relative to gravity scales asymptotically like $P_r \propto r^{(n-2.5)\alpha}$. In this context it is relevant that $n \gtrsim 2.5$ is often inferred from observations (e.g., Waters 1986), so that the radial radiative force may fall off similarly to gravity, as occurs when $n = 2.5$ since then P_r is roughly constant. It may also fall off less steeply if $n > 2.5$, since then P_r increases with radius. Note that the latter situation cannot persist to arbitrarily large radii or the disk would become unbound far enough from the star.

Thus we stress the surprising and important result that radiation that is neither radial nor azimuthal (μ equals neither 0 nor 1) induces CAK-type line forces due to the orbital gradients (recall Figure 1). Even in the absence of radial flow, incident radiation that is prograde/retrograde symmetric (i.e., symmetric in ϕ) results in a force pointing radially outward. Note that since we assumed Keplerian orbits in the derivation of equation (14), which is not strictly consistent with the presence of a radiative force, we can only use our expressions to test when the magnitude of the radiative force will represent a *small* perturbation to gravity. We quantify this comparison next.

3. Estimating the Magnitude of Radiative Forces on Circular Orbits

In the previous section, it was shown that acceleration by line forces is strongest when the density is low and self-shadowing is minimized. The first point of interest is to determine

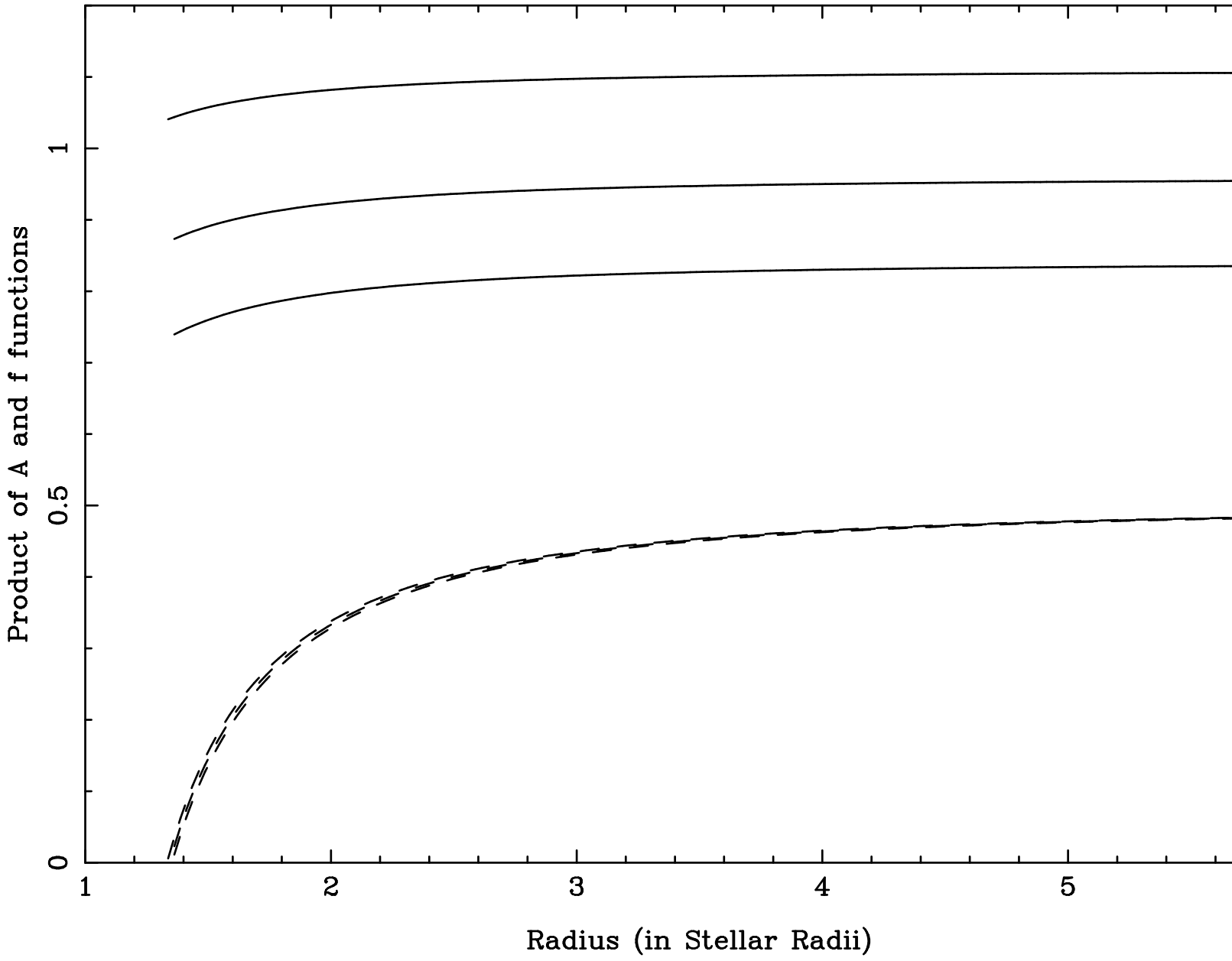

Fig. 2.— The radial dependence of the quantities $A_\alpha f_0(r)$ (solid curves) and $3/2 - f_1(r)/f_0(r)$ (dashed curves), plotted for $\alpha = 1/3, 1/2$, and $2/3$. In all cases, increasing curve height corresponds to increasing α. The dashed curve is only plotted in its positive regime, where the radiative torque has the same sign as v_r.

how low the density needs to be to enable the radiative force to compete with gravity and alter the Keplerian structure. Thus our approach of expressing the radiative acceleration as a ratio to gravity will continue to be convenient.

3.1. Radial Radiative Acceleration Compared to Gravity

To quantify this ratio, we apply equation (9) subject to equation (15). The total radial line force in units of gravity is then

$$\frac{g_r}{g_{grav}} \;=\; \Gamma(\alpha)\frac{2}{\pi}\left(\frac{3}{2}\right)^{\alpha} A_\alpha f_0(r)\Gamma Q^{1-\alpha}(GM)^{\alpha/2}R^{\alpha}\left(\rho\kappa_{es}c\right)^{-\alpha} r^{-5\alpha/2}\;. \tag{18}$$

This result, along with equation (13), shows that the overall scale of the radiative force in units of gravity is set by ΓQ times the factor $(Q\rho\kappa_{es}rc/v_\phi)^{-\alpha}$, which is quite similar to the wind result with the characteristic velocity replaced by v_ϕ.

Gayley (1995) argues that Q may canonically be of order 10^3. A careful analysis by Puls *et al.* (2000) indicates that, for effective temperatures characteritic of B-stars, the meaning of the Q parameter requires generalization. Taking their results for $T_{eff} = 20,000K$ allows us here to use an an effective value of Q, given by $Q \;=\; \bar{Q}^{1/(1-\alpha)}Q_o^{-\alpha/(1-\alpha)} \;=\; 315$ with $\alpha = 0.58$, although it is not clear how the higher densities characteristic of disk might alter this result. In any event, for line-driven wind theory to be valid, the product ΓQ must substantially exceed unity. If we assume a nominally bright type of Be star, similar to the B0V model used in Okazaki (2000), with $\Gamma = 5\times10^{-2}$ and $R = 5\times10^{11}$ cm, and a disk with rough parameters $\rho \sim 10^{-12}$ g cm^{-3}, $\kappa_{es} \sim 0.3$, and $v_\phi \sim 4\times10^7$ cm s^{-1}, then equation (18) gives that a crude estimate of the force ratio is of order $10^{1-6\alpha}$ at 2 stellar radii. This is quite sensitive to α, but may be of order several percent if α drops below 1/2, and possibly tens of percent if α drops below 1/3. The ratio can even approach order unity if a low α is combined with high Γ, high Q, and low ρ, so the potential exists for the basic structure of some Be disks to be substantially altered by optically thick line forces.

The above quantification is admittedly crude, since the appropriate assumptions in a high-density disk environment are as yet uncertain, and the line-list parameters are left here as free parameters that await future clarification. Still, the results suggest that the radiative force may at times represent an important perturbation to the gross disk structure, and consistency checks are advisable in general. This is particularly crucial in regions of lower density, such as would be found many scale heights above the disk midplane, or many stellar radii out into disks with $n > 2.5$. The former effect could have important ramifications for the lower boundary that supplies the mass and angular momentum for disk winds, while

the latter could impose an outer limit to the disk radius. Furthermore, even when the radiative force is found to be marginally negligible for the overall disk dynamics, it will have magnified importance for higher-order disk phenomena, such as the one-arm modes discussed by Okazaki (1997, 2000) and others (Papaloizou, Savonije, & Henrichs 1992), a point to which we will return in §4.

3.2. Radial Radiative Acceleration in Disks Relative to Winds

An alternative approach for characterizing the overall magnitude of the radial radiative acceleration in disks is to compare it to the acceleration of the polar stellar wind. This approach is informative because if we assume the line-list parameters in the disk are similar to those in the wind, then both the unknown line-strength parameter Q and the stellar luminosity affect the disk acceleration in the same way as the wind acceleration, and so cancel in the ratio. Also, other unknowns can be subsumed into the observed density ratio between the disk and the wind.

Some of these assumptions may be questionable, since the the higher disk density should cause a lower degree of ionization, and this is likely to *increase* the efficiency of the radiative coupling, due to the increased number of lines. In that case, we obtain only a lower limit for the radiative force on the disk, so the conclusions of this pilot study may actually represent *underestimates* of the effect. Notwithstanding these uncertainties, the disk/wind radiative acceleration ratio provides a useful reference, because without including the complications endemic to weak winds (Babel 1996), the polar wind acceleration is also constrained relative to gravity by CAK theory.

To make this comparison, we must express $\tilde{t}$ in the wind, which requires an assumption about the velocity structure. For simplicity we assume the wind velocity is proportional to $1 - R/r$, which is often termed a "$\beta = 1$" law. This implies that for a nonrotating wind, equation (14) is replaced by

$$\tilde{t}(\hat{\mathbf{n}})^{-\alpha} \;=\; (cQ\rho\kappa_{es})^{-\alpha} \left[1 \;-\frac{R}{r} \;+\; \mu^2 \left(2\frac{R}{r} - 1\right)\right]^{\alpha} \left(\frac{v_\infty}{r}\right)^{\alpha} \;. \tag{19}$$

Then we can write for the radial radiative acceleration ratio

$$\frac{g_D}{g_W} \;=\; \frac{P_D(r)}{P_W(r)} \;, \tag{20}$$

where the W and D denote wind and disk respectively. Evaluating P_D and P_W using equation (6) with equations (14) and (19) respectively then yields

$$\frac{g_D}{g_W} \;=\; X(r) \left[\frac{\rho_W(r)}{\rho_D(r)}\right]^{\alpha} \tag{21}$$

where we have defined the function

$$X(r) \;=\; \frac{2}{\pi}\left(\frac{1-\alpha}{2.1\alpha}\right)^{\alpha}(1+\alpha)A_{\alpha}f_0(r)\frac{R^{\alpha/2+1}(2R-r)r^{3\alpha/2}}{[r^{2+2\alpha}-(r^2+rR-2R^2)^{1+\alpha}]} \tag{22}$$

which encodes all the geometrical differences between Keplerian disks and radially streaming winds with $\beta = 1$. Here it has further been assumed that the stellar wind terminal speed can be characterized by the empirical relation $v_\infty/v_{esc} \cong 2.2\alpha/(1-\alpha)$ (approximated roughly from the analytic solution of Kudritzki *et al.* 1989), and neither limb- nor gravity-darkening are included.

The function $X(r)$ is plotted in Figure 3 for $\alpha = 1/3$, $1/2$, and $2/3$. Note that the decrease in X with α arises partly from the more rapid wind acceleration for high α, and partly from the details of the radiative force in the disk. More fundamentally, and contrary to the expectations (e.g., Okazaki 2000), since $X(r)$ is *not* small the magnitude of g_D/g_W is controlled primarily by the $(\rho_W/\rho_D)^{\alpha}$ factor. This expresses the fact that the self-shadowing correction reduces the acceleration substantially only if the disk has a much higher density than the wind, and, especially for low α, the geometrical differences between a Keplerian disk and a wind are not as large as might be expected. Thus the primary difference between CAK-type forces in a disk as opposed to a wind, in the single-scattering limit for the UV continuum, arises from the density difference and not the geometrical differences, and this is especially true for low α. Furthermore, when α is low, weaker lines dominate and self-shadowing is less severe, so even the density difference has a less pronounced impact.

In summary, when α and the disk density are both high, it is clear that the radiative acceleration in the disk drops significantly. On the other hand, for low α, regions of the disk which have densities comparable to the polar wind, such as may occur near its edges or at large radii, will experience a radiative acceleration that is of the same order as in the wind. We may even conclude from Figure 3 that for sufficiently small values of $\alpha \lesssim 1/3$, radiative accelerations that are of the same magnitude as those in the wind may be achieved even at depths in the disk where the density exceeds the wind density by two orders of magnitude.

The appearance of windlike accelerations at the edge of the disk is the cause of a disk wind, so these results suggest there may be a more gradual transition from a Keplerian disk into a disk wind than is generally assumed (see e.g., Proga, Stone, & Drew 1999; Feldmeier, Shlosman, & Vitello 1999). If so, the trading of centrifugal support for radiative support could reduce the specific angular momentum, and induce orbital shears and angular momentum transport in the boundary layer below the disk wind, in ways that are yet to be quantified. Future work on the effects of radiative forces on steady-state disk dynamics is planned, to elucidate the anticipated ramifications for radiatively driven mass-loss rates and the critical-point topology.

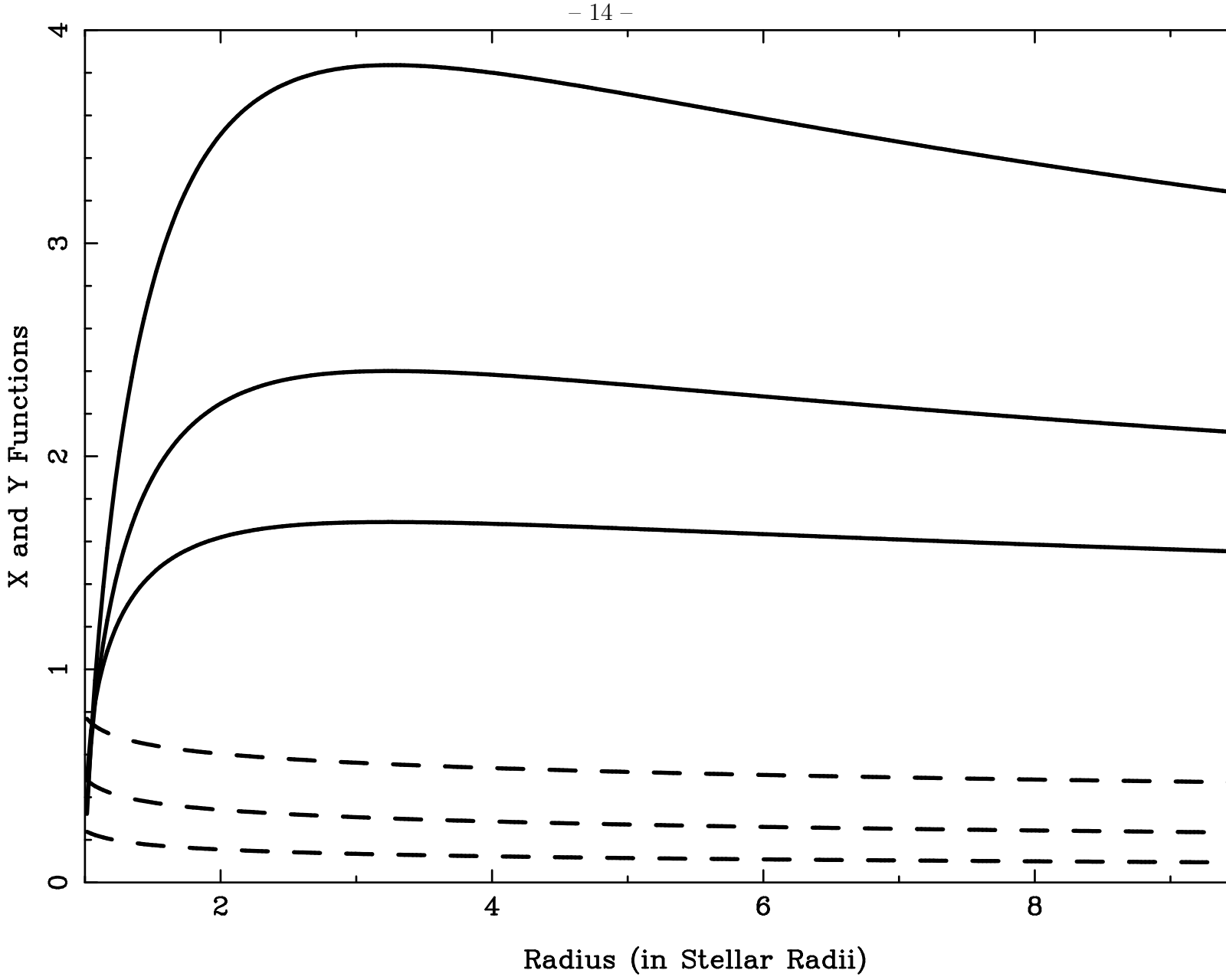

Fig. 3.— The radial dependence of the geometric functions $X(r)$ (dashed curves; the ratio of disk acceleration to wind acceleration at the same density) and $Y(r)$ (solid curves; the ratio of disk acceleration to gravity assuming windlike properties) are plotted, again for α =1/3, 1/2, and 2/3. The lower values of $X(r)$, and the higher values of $Y(r)$, are associated with higher α. (The reversal is due to the fact that $X(r)$ is influenced by the faster wind acceleration when α is high.)

Furthermore, as mentioned above, we may actually be underestimating the forces in the denser, cooler, and less ionized disk by assuming that the line list is essentially the same in the disk as in the wind. Therefore, firm constraints on the expected values of the line-opacity parameters in disks are required before disk-structure models can safely neglect the radial radiative force.

3.3. Relation to Gravity Using the Disk/Wind Density Ratio

Ultimately, the key is not how the disk acceleration compares to that in the wind, but rather how it compares to gravity. As mentioned above, expressing the radiative acceleration in the disk in terms of the acceleration in the polar stellar wind allows us another approach for comparing it to gravity, since gravity and the wind acceleration have in theory a fixed relationship. If we assume the wind is losing mass at the maximum rate consistent with the CAK formalism, this relationship is (Friend & Abbott 1986; Pauldrach, Puls, & Kudritzki 1986)

$$\frac{g_W}{g_{grav}} \;=\; \frac{(1+\alpha)F}{\alpha^\alpha(1-\alpha)^{1-\alpha}}\left(\frac{g_{net}}{g_{grav}}\right)^\alpha \;, \tag{23}$$

where g_{net} is the *actual* net acceleration of the wind and F is the "finite disk" correction factor, evaluated below. Note that at the critical point, $F \cong 1/(1+\alpha)$ and $g_W/g_{grav} = 1/(1-\alpha)$. If we again assume $v_\infty/v_{esc} \cong 2.2\alpha/(1-\alpha)$ with a $\beta = 1$ wind, then

$$\frac{g_{net}}{g_{grav}} \;=\; 9.68\frac{\alpha^2}{(1-\alpha)^2}\left(1-\frac{R}{r}\right) \tag{24}$$

and

$$\frac{g_W}{g_{grav}} \;=\; 9.68^\alpha\frac{\alpha^\alpha}{(1-\alpha)^{1+\alpha}}(1+\alpha)F\left(1-\frac{R}{r}\right)^\alpha \;, \tag{25}$$

where the finite-disk correction factor is

$$F \;=\; \frac{r^2}{(1+\alpha)R(2R-r)}\left\{1 \;-\; \left[1-\left(2-\frac{r}{R}\right)\frac{R^2}{r^2}\right]^{1+\alpha}\right\} \;. \tag{26}$$

Equation (25), coupled with equation (21), allows us to find a new expression for g_D/g_{grav}, where many of the variables in the previous equation (18) are replaced by the observable density ratio between disk and wind. The result is

$$\frac{g_D}{g_{grav}} \;=\; Y(r)\left[\frac{\rho_W(r)}{\rho_D(r)}\right]^\alpha \tag{27}$$

where

$$Y(r) \;=\; \frac{2}{\pi} 4.6^{\alpha} \frac{(1+\alpha)^2}{(1-\alpha)} A_{\alpha} f_0(r) F \frac{r^{\alpha/2} R^{\alpha/2+1} (r-R)^{\alpha} (2R-r)}{[r^{2+2\alpha} - (r^2 + rR - 2R^2)^{1+\alpha}]} \; . \tag{28}$$

In comparison with equation (18), this alternate form removes the unknown Q parameter and demonstrates explicitly the importance of the density ratio, since $Y(r) \gtrsim 1$ and varies only gradually with r and α, as shown in Figure 3.

The detailed behavior of $Y(r)$ is sensitive to the schematic choice $\beta = 1$ and is not intended to be quantitatively reliable; only its overall magnitude is significant. Note further that it is simply connected to $X(r)$ by $Y/X = g_W/g_{grav}$ (and see eq. [25]), so the fact that Figure 3 shows $Y(r)$ to be substantially larger than $X(r)$ is simply due to the fact that a CAK-type wind accelerates substantially faster than gravity (Gayley 2000). The point being made here is simply that if a Keplerian disk had the same density and line properties as a stellar wind at some r, then the azimuthally orbiting gas would actually experience a *larger* outward radiative acceleration than the radially streaming gas. This would of course invalidate the Keplerian disk assumption, and suggests that disks around UV-bright stars must have higher than windlike densities to avoid being rapidly blown off.

Since the Y function is seen to vary only over about a factor of 2 over much of the disk for a wide range in α, it is clear that the importance of the α parameter appears primarily as the exponent of the disk density, relative to canonical CAK-type winds. The fact that the disk is expected to be orders of magnitude denser than the wind indicates that this dependence on α can be quite steep. It is thus significant that Puls *et al.* (2000) argue in favor of $\alpha \sim 0.3$ in B-star winds, a fairly low value which is also supported by the low terminal speeds around these stars. If such low α is characteristic of the disk as well, we conclude that even Keplerian disks that are denser than winds by 2–3 orders of magnitude may experience line forces that modify gravity at the 10–20% level, and the potential impact on disk models should not be overlooked. This holds even for purely circular orbits; the subtle ramifications for radiative forces when orbital eccentricity appears is treated next.

4. Precession of Slightly Elliptical Orbits Due to Radiative Forces

Even when the radiative force is small compared to gravity, it can have an important cumulative effect over many orbits. Here we show that even weak radiative forces should be expected to cause precession of linear perturbations to gas parcels in circular orbit. However, substantial uncertainly remains because we find one important effect which gives rise to prograde precession while another of comparable importance leads to retrograde precession, leaving even the predicted *sign* in question.

4.1. Radiative Perturbations to First Order in Eccentricity

If slightly elliptical orbits are allowed, v_r is no longer zero, and a more complicated expression for equation (11) becomes necessary. Nevertheless, treating v_r as small compared to v_ϕ again results in a form that is convenient for analytic manipulation. To first order in v_r/v_ϕ the radial force is unaffected, but significantly, an azimuthal *torque* appears.

The presence of this torque is a subtle consequence of the angular character of Sobolev opacity, which is sensitive to the line-of-sight velocity gradient. This gradient is azimuthally asymmetric in the presence of rotation and expansion (Grinin 1978), and the resulting generation of radiative torque has been studied in the limit of *large* v_r/v_ϕ in stellar winds by Gayley & Owocki (2000). Here we consider the opposite limit, applicable to orbits with low ellipticity.

If we work to lowest order in v_r/v_ϕ, then $\tilde{t}(\hat{\mathbf{n}})^{-\alpha}$ has a different action on even and odd components of the azimuthal distribution of incident radiation. The appropriate value for $\tilde{t}^{-\alpha}$ is the same as equation (14) when applied to the *even* moment responsible for the radial force, but for the *odd* moment responsible for the azimuthal torque, it becomes (using eq. [11]) to lowest order

$$\tilde{t}_{odd}(\hat{\mathbf{n}})^{-\alpha} \;\cong\; -\left(\frac{3}{2}\right)^{\alpha-1} \alpha(1+\sigma\mu^2)\mu^{\alpha-1}(1-\mu^2)^{(\alpha-1)/2}\frac{|\sin\phi|^\alpha}{\sin\phi}\left|\frac{v_\phi}{r}\right|^\alpha \frac{v_r}{v_\phi}(cQ\rho\kappa_{es})^{-\alpha}\ , \quad (29)$$

where $\sigma = \partial \ln v_r/\partial \ln r \;-\; 1$.

4.2. Torque on Aligned Fixed-Eccentricity Orbits

The value of σ requires an assumption about the orbital geometry. Note that if $\partial v_r/\partial r \;<\; 0$, then $\sigma \;<\; -1$, and the $1+\sigma\mu^2$ term changes sign at high μ. This is an important consideration for the torque, since the prograde/retrograde symmetry is broken by the competition between the orbital expansion/compression along oblique prograde/retrograde angles, and the expansion or compression due to v_r. The radiative torque due to angles with $1+\sigma\mu^2 \;<\; 0$ has the same sign as v_r and adds angular momentum when $v_r \;>\; 0$, whereas $1+\sigma\mu^2 \;>\; 0$ removes it. Thus the value of σ controls the sense of the torque, and as we show below, the sense of the precession.

Since a one-arm mode is an azimuthally coherent structure, the major axes of the embedded elliptical orbits must align. Furthermore, the density perturbations will peak where the orbital eccentricity peaks. When the eccentricity is maximal, it is also locally constant, describing a local family of homologous orbits with a range of periastron distances.

For given eccentricity ε, the radial velocity in nearly circular orbits becomes

$$v_r \cong \varepsilon \sin\phi \sqrt{\frac{GM}{r_p}} , \tag{30}$$

where ϕ is the orbital angle measured from periastron and r_p is the periastron distance. Since r is close to r_p, equation (30) gives

$$\sigma \cong -\frac{3}{2} + \frac{d\ln\varepsilon}{d\ln r_p} , \tag{31}$$

so that $\sigma \cong -3/2$ whenever ε is slowly varying. Note that when $v_r > 0$, this also implies $\partial v_r/\partial r < 0$ (i.e., the radial velocities are convergent), despite the fact that neighboring orbits themselves are divergent. This counterintuitive behavior occurs because the angular velocity of neighboring orbits is not the same, so outer orbits lag inner ones and gas in the outer orbit does not increase in r as rapidly as gas in the inner orbit, so the radial components of the individual gas parcels converge even as their orbital traces diverge.

Using $\sigma = -3/2$ and equation (29) in equations (6) and (9), we thus find that the (small) azimuthal acceleration owing to the radiative torque is

$$g_\phi = g_{grav}\Gamma Q \Gamma(\alpha) P_\phi \tag{32}$$

where

$$P_\phi = \frac{2^{2-\alpha}3^{\alpha-1}}{\pi}\alpha A_\alpha \left[\frac{3}{2}f_0(r) - f_1(r)\right](Q\kappa_{es}c\rho)^{-\alpha}\left(\frac{R}{r}\right)^\alpha \left|\frac{v_\phi}{r}\right|^\alpha \frac{v_r}{v_\phi} . \tag{33}$$

Note that the torque is proportional to v_r, a convenient property we will exploit below. Like the coriolis force in the nearly corotating frame, this has the important ramification that the sign of the torque reverses when v_r reverses, so the torque is applied antisymmetrically and thus imparts no net angular momentum over a complete cycle between turning points. In the presence of this torque the orbits are no longer strictly elliptical, and indeed do not close on themselves, but the energy and angular momentum become periodic functions of r, so $r(t)$ remains periodic. The small deviation from Keplerian motion can then only yield orbital *precession*.

The assertion that the motion is symmetric about the turning points follows from the fact that the force depends only on radius and velocity and is invariant under time reversal. Thus bounded motion must progress from turning point to turning point in the same way regardless of whether time runs forward or backward, so there is no hysteresis and $r(t)$ is periodic. The time reversibility is obvious for the *magnitude* of optically thick radiative forces, which in the Sobolev approximation depend only on the magnitude of the line-of-sight velocity gradient. This invariance also applies to the *sign* of the radiative torque, because

equation (32) shows that reversing the radial velocity v_r changes the sign of the torque *relative* to the azimuthal velocity v_ϕ, which is itself reversed.

The lack of hysteresis between turning points does not imply that the "orbits" are closed, because the azimuthal angle covered in each full cycle is not necessarily equal to 2π. Instead, in the presence of torque, the apsides will precess. Before calculating this precession, we first quantify the radiative torque magnitude by comparing it to the lateral force that is responsible for maintaining closed orbits in the rotating frame, namely the coriolis force.

4.3. Magnitude of the Radiative Torque Relative to the Coriolis Force

The coriolis force in the corotating frame of a nearly circular orbit gives a fictitious azimuthal acceleration

$$g_{cor} \;=\; -2\Omega_p v_r \tag{34}$$

for Ω_p the orbital angular velocity at periastron for nearly circular Keplerian orbits. Note that g_{cor}, like the radiative g_ϕ, is proportional to v_r, so a simple ratio exists, which from equation (29) applied in equation (6) is given by

$$\frac{g_\phi}{g_{cor}} \;=\; -\Gamma(\alpha)\alpha\left(\frac{3}{2}\right)^{1-\alpha} A_\alpha \Gamma Q \left(\frac{|v_\phi|}{cQ\rho\kappa_{es}r}\right)^\alpha \sqrt{\frac{r}{R}}\int_{\mu_*}^1 d\mu\ \mu^{\alpha-1}(1-\mu^2)^{\alpha/2}\ . \tag{35}$$

4.4. Precession Due to Torque Proportional to Radial Speed

We wish to quantify the precession of a homologous (constant eccentricity) family of slightly elliptical orbits of gas parcels, all with the same major axis direction so the family yields a coherent density perturbation. It is not necessary to solve the equations of motion; the behavior is specified by solving for the energy and angular momentum alone. Note that here these quantities are not constant within a given orbit because of the work and the torque applied by the radiative force.

It is convenient to write equation (32) in the simple form

$$g_\phi \;=\; \frac{\Omega}{N_\phi} v_r\ , \tag{36}$$

where $\Omega = v_\phi/r = \sqrt{GM/r^3}$ is the angular velocity of the orbit to lowest order. Here the key parameter

$$N_\phi \;=\; \frac{\pi}{\Gamma Q^{1-\alpha}\Gamma(\alpha)2^{2-\alpha}3^{\alpha-1}\alpha A_\alpha\left[\frac{3}{2}f_0(r)-f_1(r)\right]}(c\kappa_{es}\rho)^\alpha\left(\frac{r}{R}\right)^\alpha\left(\frac{r^3}{GM}\right)^{\alpha/2} \tag{37}$$

remains approximately constant over nearly circular orbits, and the Appendix shows that it can be interpreted as the number of nearly-closed orbits required for a full precession cycle, due to the effects of the torque alone. If its sign is positive, precession is prograde, and if negative, retrograde. This distinction depends on r and σ, but in typical cases of interest ($r \gtrsim 2R$, $\sigma \cong -1.5$), the radiative torque yields positive N_ϕ and contributes to prograde precession.

To estimate the magnitude of the precession rate, we again consider $Q = 315$ and $\alpha = 0.58$, and adopt similar parameters for a B0V star as used by Okazaki (2000) with $\Gamma = 4.5 \times 10^{-2}$, $M = 17.8$ M$_\odot$, $r = 5.2 \times 10^{11}$ cm, and a disk density of $\rho = 10^{-12}$ gm cm^{-3}. With equation (37), these yield $N = 637$ at roughly 3 stellar radii, corresponding to a precession period of 5.3 years. Observed precession periods are also of order a few years (Mennickent, Sterken, & Vogt 1997), and the few whose orbital sense is known are all prograde, so this suggests that radiative torque may be an important contributor. However, we will show next that a competing effect also exists which may act to reverse the sign of radiatively induced precession.

4.5. Precession Caused by Non-Inverse-Square Radial Acceleration

The presence of slight ellipticity not only induces torques, it implies that r, and therefore the radiative force, changes over the course of an orbit. If such changes differ from an inverse-square force law, they also cause precession, in a manner similar to a quadrupole moment of gravity (Papaloizou, Savonije, & Henrichs 1992). To discover the magnitude of this effect, it is convenient to write the radial radiative force in the form

$$g_r \;=\; g_{grav} \frac{2}{(2 - m_{rad})} \left(\frac{r}{r_p} \right)^{-m_{rad}} \frac{1}{N_r} \;, \tag{38}$$

where r_p is the periastron radius and

$$m_{rad} \;=\; \frac{d \ln g_r}{d \ln r} \tag{39}$$

governs the gradient of g_r *over a single elliptical orbit* (i.e., for a fixed periastron distance r_p). In the Appendix, it is shown that N_r may be interpreted as the number of orbits per precession cycle, due solely to the gradient in g_r over an orbit. Note that negative values for N_r imply retrograde precession and occur whenever $m_{rad} > 2$.

The determination of m_{rad} depends on the density gradient over one orbit, as well as on the assumed eccentricity gradient, since the latter thus controls the gradient in velocity

between neighboring orbits. The simplest assumption is that neighboring orbits have the same eccentricity, which is applicable near eccentricity extrema. Assuming that such extrema are also relevant to the behavior of global modes allows our results to be suggestive for global mode precession as well, although a self-consistent calculation is needed. Furthermore, we assume the lines of nodes of all orbits are aligned, so similar elliptical orbits are embedded in a simple way to form our approximation to the behavior of a global mode.

If it is also assumed that the temperature does not vary, fixed eccentricity implies that $\rho \propto r^{-1}$ over an orbit, because conservation of angular momentum implies a compression that is proportional to r, which cancels the r^{-1} dependence from the stretching in the vertical direction due to the rising scale height, which leaves only the radial r^{-1} stretching due to the similarity of the nested ellipses. Meanwhile, the remaining geometric effects involving the flux integral over the line-of-sight velocity gradient indicates that $g_r \propto \rho^{-\alpha} r^{-5\alpha/2}$, if we neglect the weak variations in $f_0(r)$ (see eq. [15]). Thus we obtain for aligned orbits with constant eccentricity

$$m_{rad} \;=\; 2 \;+\; \frac{3\alpha}{2} \;, \tag{40}$$

and so equation (38) with $g_{grav} = r\Omega^2$ implies

$$N_r \;=\; -\frac{4}{3\alpha}\frac{r\Omega^2}{g_r} \tag{41}$$

gives the number of orbits per (retrograde) precession cycle, due solely to the radiative force gradient. This expression may be callibrated by comparison with eq. (18).

4.6. Degree of Cancellation of Radiative Precession Effects

We have seen that at most radii, the torque effect by itself would yield prograde precession, while the radiative gradient effect would yield retrograde. Since these two effects are of similar order, they compete, and a substantial degree of cancellation occurs. How this would affect a coherent one-arm mode has yet to be calculated, but in the situation considered here, that of aligned fixed-eccentricity orbits with no gas pressure, it is straightforward to show that the gradient effect is the larger of the two. This can be seen by considering the ratio N_ϕ/N_r, which due to equations (36) and (41) can be written

$$\frac{N_\phi}{N_r} \;=\; -\frac{4}{3\alpha}\frac{P_\phi v_\phi}{P_r v_r} \;. \tag{42}$$

Then equations (15) and (33) further imply

$$\frac{N_\phi}{N_r} \;=\; -\frac{8}{9}\left(\frac{3}{2} \;-\; \frac{f_1(r)}{f_0(r)}\right) \;. \tag{43}$$

An asymptotic analysis reveals that in the limit of large r/R, this becomes

$$\frac{N_\phi}{N_r} \cong -\frac{4}{9}\left[1 - \frac{(4+2\alpha)}{(4+\alpha)}\frac{R^2}{r^2}\right] . \tag{44}$$

Thus N_ϕ/N_r has little α sensitivity at large radii, stemming from the weak α sensitivity of $f_1(r)/f_0(r)$. The competition between prograde and retrograde precession has an intrinsic character that is nearly independent of the line distribution.

Since the smaller the precession number N the stronger the effect, equation (44) implies that at large radii the gradient effect is marginally dominant, yielding a net retrograde precession. Of course, for $r \lesssim 1.3R$ where the dashed curves in Figure 2 go negative, the torque effect also yields retrograde precession. Thus the results here predict retrograde precession is always the result of line forces in the limit of small perturbations from circular orbits, when the orbital eccentricities are co-aligned and constant.

The quantitative results for N_ϕ and $-N_r$, converted into timescales by multiplying by the orbital periods for the characteristic stellar parameters listed above, are independently graphed in Figure 4. The ratio between the curves can be seen to agree with equation (43), and the magnitudes are seen to roughly correspond to yearlike timescales. Also plotted is the result for the quadrupole precession effect on similar orbits for the parameters in Papaloizou, Savonije, & Henrichs (1992), where it can be seen that radiative effects may compete quite effectively with the prograde precession caused by gravitational perturbation.

Although this analysis does not guarantee that a coherently growing mode including pressure forces would also show retrograde precession, it suggests that the radiative effects on such a mode would include two separate and competing terms of similar magnitude, and retrograde precession seems a possible outcome. That observations typically show prograde precession suggests that either the quadrupole correction to gravity dominates (see the Appendix), or that the radiative effects in a one-arm mode are not well modeled by small fixed-eccentricity modifications to circular orbits. One suggestion that the latter could be true is that the observed amplitudes of one-arm modes (Hummel & Hanuschik 1997) are often not small, and would fall well outside the linear regime treated here. Future nonlinear calculations are needed, perhaps advancing on the analytic work of Lee & Goodman (1999). The magnitude of the results here indicate that optically thick line forces should be included in any future such effort.

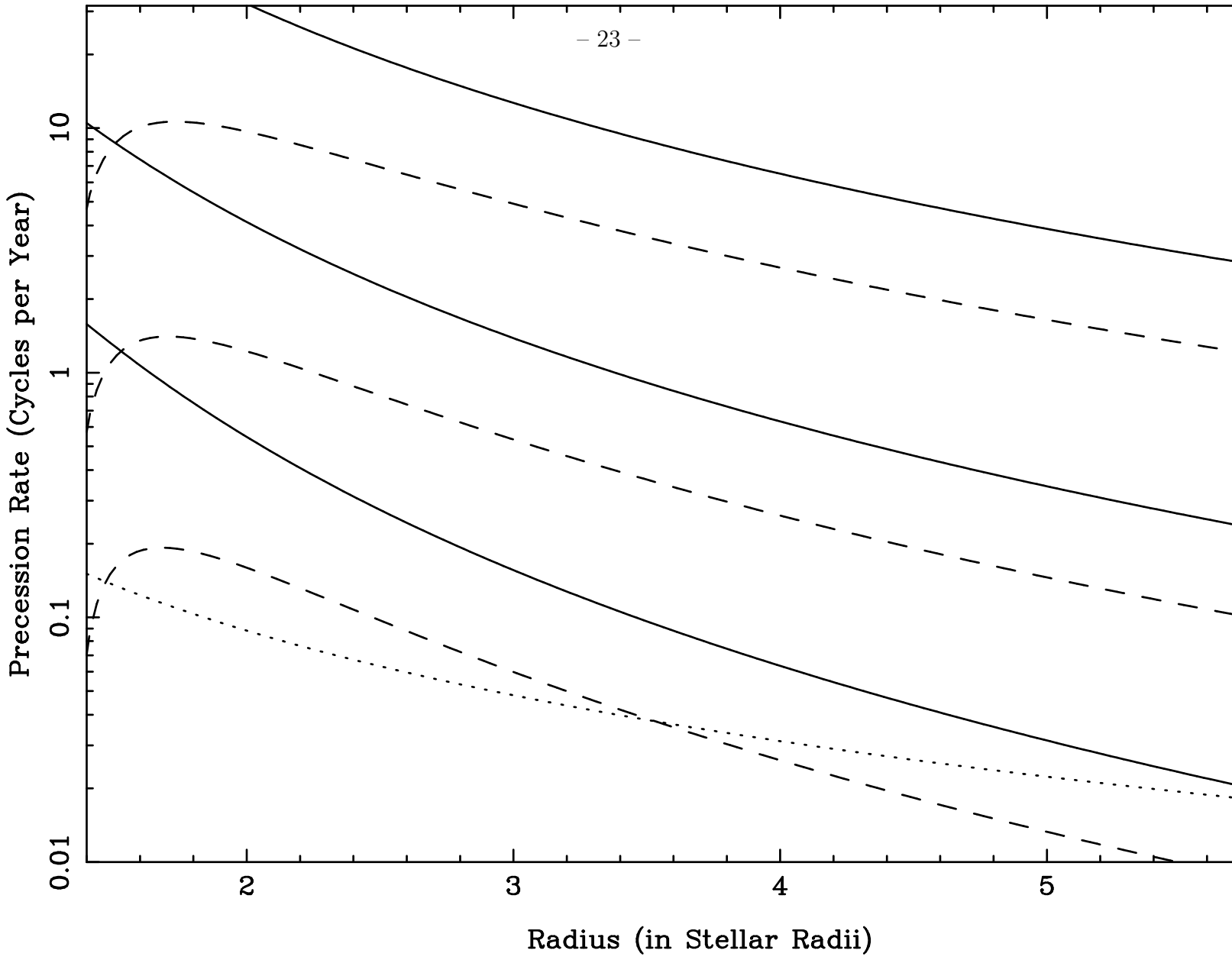

Fig. 4.— The rates of retrograde precession due to the gradient effect (solid curves) and prograde precession due to the torque effect (dashed curves) are plotted as functions of radius of the individual orbits, for the stellar parameters in the text, again using $\alpha = 1/3$, $1/2$, and $2/3$. In both the solid and dashed sequences plotted, faster precession rates correspond to lower α. Also plotted for comparison is the prograde precession rate due to the quadrupole correction to gravity (dotted curve) taken from the model parameters in Papaloizou, Savonije, & Henrichs (1992). As shown in the Appendix, the combined precession rate is found by simply adding the contributions, where retrograde rates (solid curves) are negative. There is no global mode present, the rates are for individual slightly elliptical orbits with no gas-pressure coupling.

5. Conclusions

This paper argues that partially optically thick line forces are a potentially important contributor to the force balance in Keplerian disks orbiting Be stars, and other analogous UV-bright enviroments. The neglect of line forces in such disks in the past is probably due to a conceptual bias toward point stars and radial radiation streams, which would not encounter velocity gradients and would not yield important line forces. However, finite stellar disks produce nonradial radiation streams that do encounter supersonic velocity gradients even when there is no radial velocity at all. The zeroth-order effects on disk structure may be negligible in high-density regions unless $\alpha \lesssim 0.3$, but will likely become important near the disk boundaries, where the densities are lower and closer to windlike. This could yield important complications for disk winds, which might emanate from disk material that requires a lower specific angular momentum to be in orbit once radiative levitation is included. Also, there can be an impact on the farther reaches of the disk where the density is thought to drop steeply. Finally, there are also important implications about the difficulty of building a disk slowly from initially low densities, since the gas might not be containable against radiative driving unless the density is high enough to yield substantial self-shadowing in the lines. Consequently, if constant line parameters are adopted, the radiative force has greater impact for lower density, lower α, and higher Γ.

A central conclusion is that, notwithstanding uncertainties in the appropriate parameters, the similarities in the driving efficiency in a wind and in a disk strongly suggest that, in the absence of additional disk confinement such as from magnetic fields, it should not be possible to support a *low*-density Keplerian disk at the equator *and* a line-driven wind over the poles at the same time. High-density disks, on the other hand, can avoid being blown off like the polar winds only by virtue of their reduction of line driving by self-shadowing. As speculated by Marlborough (1997), non-steady mass input might occur for Be disks in a process similar to miniature LBV eruptions. Perhaps this could help increase the disk densities during their vulnerable formation epoch.

Furethermore, the potentially unstable role of self-shadowing in the presence of nonlinear disk dynamics suggests that radiative stripping of the disk might be able to occur more catastrophically than the typical steady disk-wind model. If so, it could contribute to the commonly seen disappearances of disks, although no such mechanism is offered here because of its inherently nonlinear nature. This is highly speculative, but the possibility that nonsteady mass input to and output from a disk may involve line driving justifies further studies into the role of radiative forces in circumstellar disks.

In addition, higher-order forces, such as the effects of gas pressure, quadrupole gravity terms, and viscosity, should receive strong competition from radial radiative forces, and also

from radiative torques for noncircular orbital perturbations. Furthermore, the combined effect of radiative torque and radial radiative force on a locally aligned family of slightly elliptical orbits of fixed eccentricity is to induce precession, and for suitable parameters the timescales can be comparable to observations. However, it is significant that the two effects are typically of similar magnitude but opposite sign, and therefore compete. The simple models calculated here predict that the retrograde precession due to the force gradient should be stronger than the prograde precession due to the torque effect, contrary to observations which favor prograde precession of nonlinearly developed one-arm modes. The degree of cancellation between these effects might also contribute to the apparent stochasticity of observed precession rates.

It must be cautioned that all precession rates inferred here are entirely schematic, since no global modes are included. Eigenvalue calculations are needed to ascertain the impact on the formation and evolution of small-amplitude one-arm modes, and numerical calculations are needed to follow these into the nonlinear regime. However, the results here suggest that dynamically sensitive line forces can play an important role in such calculations, and should be included.

The quantitative reliability of all these conclusions is limited by the current uncertainties in the line parameters in a Be-star disk, and by the absence of nonlinear hydrodynamic simulations that include the radiative force. The main purpose of this paper has been simply to categorize how these forces might be expected to alter disk morphology, using an analysis of nearly circular orbits. The extremely variable behavior of Be-star disks indicates that additional physics will be required to understand them, but it seems likely that radiative forces will play a role in any complete description, especially for the hotter and brighter stars. The possibility also exists to extend these results to other UV-bright quasi-Keplerian disks, such as accretion disks. Recent advances in hydrodynamic modeling offer promise for future developments, as long as the potential role of line forces is properly considered.

The authors would like to acknowledge helpful and interesting discussions with Jon Bjorkman and Karen Bjorkman. This work was supported in part by NASA grants NAG5-3530 and NAG5-4065.

6. Appendix

Here we derive the results, used in the text, that a torque proportional to v_r yields prograde precession over N_ϕ orbits, with

$$N_\phi \;=\; \frac{\Omega v_r}{g_\phi} \;=\; \frac{1}{2}\frac{g_{cor}}{g_\phi}\;, \tag{45}$$

whereas a radial acceleration that is proportional to $r^{-m_{rad}}$ over an orbit yields retrograde precession over N_r orbits, with

$$N_r \;=\; \frac{2}{(2-m_{rad})}\frac{r\Omega^2}{g_r} \;=\; \frac{2}{(2-m_{rad})}\frac{g_{grav}}{g_r}\;. \tag{46}$$

As in the text, $\Omega \;=\; \sqrt{g_{grav}/r}$ is the orbital frequency, and $g_{cor} = 2\Omega v_r$ is the magnitude of the coriolis force. The sign convention is that positive N implies prograde precession, which holds for N_ϕ at suitably large radii, and for N_r if $m_{rad} < 2$.

The key expression for the azimuthal angle traced out during one passage from the inner turning point r_p to the outer turning point r_a can be written

$$\Delta\phi = \int_{r_p}^{r_a} dr\; \frac{l(r)}{r^2 v_r}\;, \tag{47}$$

where $l(r)$ is the specific angular momentum of the gas parcel. This equation derives directly from $d\phi/dr = v_\phi/(rv_r)$ and $v_\phi = l/r$. The extent of the prograde or retrograde precession in each orbit depends on how much $\Delta\phi$ is greater or less than π. The limits of the integration are the turning points where $v_r = 0$, which is where the denominator is singular. This singularity requires that the expression be evaluated carefully.

The radial speed v_r is inferred from the energy equation, including the work done by gravity, by the radial radiative force, and by the radiative torque. To accomodate the effects of precession due to a quadrupole moment, we split gravity into its usual point-mass form $g_{grav} = -GM/r^2$ plus a quadrupole correction $-f_q$ which scales as r^{-4}, where the sign of f_q is explicitly positive. The radial radiative acceleration is denoted f_r, which varies both as a function of r_p and r, where r_p is the periastron distance of the orbital path in question, and r specifies the varying location *along* that path. Thus variations from orbit to orbit are kept track of *separately* from the variation over a given orbit. In the same spirit, we further define two functions that vary over an orbit and are necessary to accomodate the torque effect, which are

$$f_l(r) \;=\; \frac{l_p r}{r_p^2}\frac{g_\phi}{v_r} \tag{48}$$

and

$$f_\phi(r) \;=\; \frac{l(r)}{r}\frac{g_\phi}{v_r} \;, \tag{49}$$

where the subscript p applies to quantities that are held fixed over the orbit, say at their periastron values. These functions will emerge shortly as key integrands for the angular momentum and the kinetic energy, respectively.

The torque equation then allows us to specify $l(r)$ over an orbit as

$$l(r) \;=\; l_p \;+\; \frac{r_p^2}{l_p}\int_{r_p}^{r} dr'\; f_l(r') \;, \tag{50}$$

and the work integral then gives

$$\frac{1}{2}\left(v_r^2 \;+\; v_\phi^2\right) \;=\; \frac{l_p^2}{2r_p^2} \;-\; \frac{l(r)^2}{2r^2} \;+\; \int_{r_p}^{r} dr'\; \left[g_{grav}(r') \;-\; f_q(r') \;+\; f_\phi(r') \;+\; f_r(r')\right] \;. \tag{51}$$

The approach now is to substitute using equation (50) and then write an expression for the product rv_r, which can be written as a quadratic in r if all terms of order the (small) force corrections f_l, f_ϕ, f_r and f_q are Taylor expanded to second order in the small quantity $r - r_p$. Since all four f functions appear only as integrands, a second-order expansion merely requires specifying their first derivatives f', and we obtain

$$rv_r \;=\; \sqrt{r-r_p}\sqrt{r_a-r}\sqrt{\frac{2GM}{r_p} \;-\; \frac{l_p^2}{r_p^2} \;+\; r_p^2(f_l'-f_\phi') \;-\; 4r_p(f_\phi+f_r-f_q) \;-\; r_p^2(f_r'-f_q')} \;, \tag{52}$$

where the apastron distance r_a is to order f'

$$r_a \;=\; r_p\left[\frac{l_p^2 \;-\; 2r_p^3 f_l \;+\; r_p^4 f_l' \;-\; 2r_p^3(f_\phi+f_r-f_q) \;-\; r_p^4(f_\phi'+f_r'-f_q')}{2GMr_p \;-\; l_p^2 \;+\; r_p^4 f_l' \;-\; 4r_p^3(f_\phi+f_r-f_q) \;-\; r_p^4(f_\phi'+f_r'-f_q')}\right] \;. \tag{53}$$

All this allows us to write equation (47) to lowest nontrivial order in the form

$$\Delta\phi \;\cong\; \frac{l_p}{\sqrt{l_p^2 - 2r_p^3 f_l + r_p^4 f_l' - 2r_p^3(f_\phi+f_r-f_q) - r_p^4(f_\phi'+f_r'-f_q')}}\int_{r_p}^{r_a}\frac{dr}{r}\;\frac{\sqrt{r_a-r_p}}{\sqrt{r-r_p}\sqrt{r_a-r}} \;, \tag{54}$$

where the elementary integral on the right simply yields π. As a check, note that if all f functions become negligibly small we recover the purely Keplerian result of π radians between turning points. If we further define N to be the number of orbits per precession cycle, then $\Delta\phi \;=\; \pi(1-1/N)$, where $N > 0$ implies prograde precession. Expanding equation (54) then yields to lowest order

$$N \;\cong\; r_p\Omega_p^2\left[f_l \;+\; f_\phi \;+\; f_r \;-\; f_q \;+\; \frac{r_p}{2}(f_\phi' - f_l' + f_r' - f_q')\right]^{-1} \;, \tag{55}$$

where $\Omega_p = l_p/r_p^2$ is the orbital angular velocity.

Thus all that remains is to evaluate the f functions and their derivatives. In present context, we have $f_\phi = f_l r_p^2/r^2$, so $f'_\phi - f'_l = -2f_l/r_p$ and $f_l = f_\phi$ when evaluated at r_p, so we obtain simply

$$N = \frac{2r_p\Omega_p^2}{\left[2(f_l + f_r - f_q) + r_p(f'_r - f'_q)\right]} . \tag{56}$$

The values of f_l and f_r at r_p can be obtained by substituting equations (18) and (32) into equations (48) and (49) respectively. If we also define the exponent m_{rad} as the negative logarithmic derivative of f_r with respect to r at r_p, such that

$$m_{rad} = -\frac{r_p f'_r}{f_r} , \tag{57}$$

then we have $2f_r + r_p f'_r = (2 - m_{rad})f_r$. For the gravitational correction, f_q arises from knowledge of the quadrupole moment of the stellar mass, and $f'_q = -4f_q/r_p$. Replacing periastron quantities with local values, we finally find

$$N = \frac{2r\Omega^2}{[2f_l + (2 - m_{rad})f_r + 2f_q]} \tag{58}$$

as the local expression for the precession period of embedded orbits with constant eccentricity and parallel lines of nodes.

The denominator in equation (58) clearly specifies the separate precessional influences of radiative torque, radial radiative forces, and quadrupole effects. Since a positive N implies prograde precession, the torque effect yields prograde precession whenever the coefficient of v_r in g_ϕ (see eqs. [32] and [33]) is positive. The influence of radial gradients only yields prograde precession in limited cases where $m_{rad} < 2$, i.e., when the radiative force falls off more slowly than gravity as a gas parcel moves over an eccentric orbit. By contrast, the quadrupole term always yields prograde precession.

The fact that observed precession periods correspond to $\sim 10^3$ orbital periods at several stellar radii into the disk, coupled with equation (58), implies that the precession may be caused either by a non-inverse-square force with a magnitude of about 10^{-3} that of gravity, or else by an azimuthal force of this same magnitude multiplied by the ratio v_r/v_ϕ. Either way, the force perturbation must be quite small. This supports the likelihood that radiative forces over the bulk of the disk are indeed small, but does not preclude their potential to be large in regions of low density.

References

Babel, J. 1996, A&A, 309, 867

Batchelor, G. K. 1967, An Introduction to Fluid Dynamics (Cambridge: Cambridge Univ. Press), 598

Berio, P., Stee, Ph., Vakili, F., Mourard, D., Bonneau, D., Chesneau, O., Thureau, D., & Hirata, R. 1999, A&A, 345, 203

Castor, J. I., Abbott, D. C., & Klein, R. I. 1975, ApJ, 195, 157 (CAK)

Chen, H, & Marlborough, J. M. 1994, ApJ, 427, 1005

Cranmer, S. R. & Owocki, S. P. 1996, ApJ, 462, 469

Cranmer, S. R. & Owocki, S. P. 1995, ApJ, 440, 308

Cranmer, S. R., Smith, M. A., & Robinson, R. D. 2000, ApJ, 537, 433

Dachs, J. 1987, in Physics of Be stars, Proceedings of the Ninety-second IAU Colloquium, ed. A. Slettebak and T. Snow (Cambridge: Cambridge Univ. Press), p. 149

Drew, J. E. & Proga, D. 2000, NewAR, 44, 21

Feldmeier, A., Shlosman, I., & Vitello, P. 1999, ApJ, 526, 357

Friend, D. B., & Abbott, D. C. 1986, ApJ, 311, 701

Gayley, K. G. 1995, ApJ, 454, 410

Gayley, K. G. 2000, ApJ, 529, 1019

Gayley, K. G., & Owocki, S. P. 2000, ApJ, 537, 461

Grinin, A. 1978, Sov. Astr., 14, 113

Hanuschik, R. W. 1994, Ap&SS, 216, 99

Hanuschik, R. W., Hummel, W., Dietle, O., & Sutorious, E. 1995, A&A, 300, 163

Hubert, A. M. 1994, in IAU Symp. 162, Pulsation, Rotation and Mass Loss in Early-Type Stars, ed. L. A. Balona, H. F. Henrichs, & J. M. Le Contel (Dordrecht: Reidel), 341

Hummel, W. & Hanuschik, R. W. 1997, A&A, 320, 852

Hummel, W. & Vrancken, M. 2000, A&A, 359, 1075

Utrecht.

Kudritzki, R. P., Pauldrach, A., Puls, J., & Abbott, D. C. 1989, A&A, 219, 205

Herrero, A. 1999, A&A, submitted

Lee, E. & Goodman, J. 1999, MNRAS, 308, 984

Marlborough, J. M. 1997, A&A, 317, L17

Mennickent, R. E., Sterken, C., & Vogt, N. 1997, A&A, 326, 1167

Okazaki, A. T. 1991, PASJ, 43, 75

Okazaki, A. T. 1996, PASJ, 48, 305

Okazaki, A. T. 1997, A&A, 318, 548

Okazaki, A. T. 2000, The Be Phenomenon in Early-Type Stars, eds. M. A. Smith, H. F. Henrichs, and J. Fabregat

Owocki, S. P., Cranmer, S. R., Gayley, K. G. 1996, ApJ, 472, L115.

Papaloizou, J. C., Savonije, G. J., & Henrichs, H. F. 1992, A&A 265, L45

Pauldrach, A.W.A., Puls, J. & Kudritzki, R.-P. 1986, A&A, 164, 86

Proga, D., Stone, J., & Kallman, T. R. 2000, ApJ, 543, 686

Puls, J., Springmann, U., & Lennon, M. 2000, A&AS, 141, 23

Quirrenbach, A., Bjorkman, K. S., Bjorkman, J. E., Hummel, C. A., Buscher, D. F., Armstrong, J. T., Mozurkewich, D., Elias, N. M. II, & Babler, B. L. 1997, ApJ, 479, 477

Rivinius, Th., Baade, D., Stefl, S., Stahl, O., Wolf, B., & Kaufer, A. 1998, A&A, 333, 125

Robinson, R. D. & Smith, M. A. 2000, 540, 474

Smith, M. A., Grady, C. A., Peters, G. P., & Feigelson, E. D. 1993, ApJ, 409, L49

Telting, J. H., Waters, L. B. F. M., Roche, P., Boogert, A. C. A., Clark, J. S., de Martino, D., Persi, P. 1998, MNRAS, 296, 785

Telting, J. H., Heemskerk, M. H. M., Henrichs, H. F., & Savonije, G. J. 1994, A&A, 288, 558

Vakili, F., Mourard, D., Stee, Ph., Bonneau, D., Berio, P., Chesneau, O., Thureau, N., Morand, F., Labeyrie, A., Tallon-Bosc, I. 1998, A&A, 335, 261

Waters, L. B. F. M. 1986, A&A, 162, 121

Waters, L. B. F. M. & Marlborough, J. M. 1994, in IAU Coll. 162, 399

Wood, K., Bjorkman, K. S., & Bjorkman, J. E. 1997, ApJ, 477, 926